

Threshold photoelectron photoion coincidence study of the fragmentation of valence states of $\text{CF}_3\text{-CH}_3^+$ and $\text{CHF}_2\text{-CH}_2\text{F}^+$ in the range 12–24 eV[†]

Weidong Zhou,[‡] D. J. Collins,^b R. Y. L. Chim,^a D. P. Secombe[§] and R. P. Tuckett^{*a}

^a School of Chemistry, University of Birmingham, Edgbaston, Birmingham, UK, B15 2TT.

E-mail: r.p.tuckett@bham.ac.uk; Fax: +44 121 414 4403

^b Department of Physics, Reading University, Reading, UK, RG6 2AF

Received 26th March 2004, Accepted 27th April 2004

First published as an Advance Article on the web 17th May 2004

Using tunable vacuum-ultraviolet radiation from a synchrotron source, threshold photoelectron photoion coincidence spectroscopy has studied the unimolecular decay dynamics of the valence electronic states of $\text{CF}_3\text{-CH}_3^+$ and $\text{CHF}_2\text{-CH}_2\text{F}^+$. Threshold photoelectron spectra and fragment ion yield curves of $\text{CF}_3\text{-CH}_3$ and $\text{CHF}_2\text{-CH}_2\text{F}$ have been recorded in the range 12–24 eV, electrons and ions being detected by a threshold electron analyser and a linear time-of-flight mass spectrometer, respectively. For the dissociation products of $(\text{CF}_3\text{-CH}_3^+)^*$ and $(\text{CHF}_2\text{-CH}_2\text{F}^+)^*$ formed *via* cleavage of a single covalent bond, the mean translation kinetic energy releases have been measured and compared with the predictions of statistical and impulsive mechanisms. *Ab initio* G2 calculations have determined the minimum energies of $\text{CF}_3\text{-CH}_3$ and $\text{CHF}_2\text{-CH}_2\text{F}$ and their cations, with their geometries optimised at the MP2(full)/6-31G(d) level of theory. The nature of the valence orbitals of both neutral molecules has also been deduced. Enthalpies of formation of both titled molecules and all fragment ions and neutrals observed by dissociative photoionisation have also been calculated. Combining all experimental and theoretical data, the fragmentation mechanisms of the ground and excited states of $\text{CF}_3\text{-CH}_3^+$ and $\text{CHF}_2\text{-CH}_2\text{F}^+$ are discussed. The ground state of both ions, formed by electron removal from the C–C σ -bonding highest occupied molecular orbital, is stable only over a narrow range of energies in the Franck–Condon region; it dissociates by C–C bond cleavage with a small fractional translational energy release. Low-lying excited states of both ions, produced by electron removal from F 2p π nonbonding orbitals, show some evidence for isolated-state behaviour, with impulsive dissociation by cleavage of a C–F bond and a larger fractional translational energy release into the two fragments. For energies above *ca.* 16 eV smaller fragment ions, often resulting from cleavage of multiple bonds and HF elimination, are observed; for both molecules with $h\nu > 18$ eV, CF-CH_2^+ is the dominant fragment ion. New experimental values are determined for the enthalpy of formation at 298 K of $\text{CF}_3\text{-CH}_3$ (-751 ± 10 kJ mol⁻¹) and $\text{CHF}_2\text{-CH}_2\text{F}$ (-671 ± 12 kJ mol⁻¹), with upper limits being determined for $\text{CF}_2\text{-CH}_3^+$ ($\leq 546 \pm 11$ kJ mol⁻¹) and $\text{CHF-CH}_2\text{F}^+$ ($\leq 663 \pm 13$ kJ mol⁻¹).

1. Introduction

An international effort is underway to replace chlorofluorocarbons (CFCs) with environmentally-acceptable alternatives,^{1–3} and hydrofluorocarbons (HFCs) are likely to become the accepted CFC replacement in many industrial applications. Specifically, several fluorinated ethanes are already being used, including 1,1 difluoroethane (R152a), 1,1,1,2 tetrafluoroethane (R134a) and pentafluoroethane (R125). 1,1,1,2 tetrafluoroethane, for example, has been used for many years as a replacement for CF_2Cl_2 in air-conditioning systems of cars.⁴ HFCs are being used as CFC alternatives because they lack the chlorine atoms which catalyse the depletion of ozone from the stratosphere. HFCs still pose an environmental threat as they contribute to global warming,⁵ but the presence of C–H bonds cause them to react faster than CFCs with OH radicals, thereby reducing their lifetime in the earth's atmosphere. The rate constant at room temperature for the reactions of the two titled HFCs with OH is *ca.* 1.2×10^{-15} (for $\text{CF}_3\text{-CH}_3$) and 1.6×10^{-14} (for $\text{CHF}_2\text{-CH}_2\text{F}$) cm³ molecule⁻¹ s⁻¹, respec-

tively.^{6,7} The atmospheric lifetime of these two trifluoroethanes will then be as low as *ca.* 25 or 2 years, assuming an average OH concentration of 10^6 molecule cm⁻³. Removal by photoionisation and photodissociation processes in the mesosphere, therefore, is only likely to play a small role in the overall loss of these molecules from the atmosphere, and is unlikely to be dominant. However, a knowledge of the vacuum-UV (VUV) photochemistry of HFCs that might take place in this region of the atmosphere is needed, and might be important in the determination of the atmospheric lifetime.

Our group is investigating the decay dynamics of halocarbon and HFC cations containing at least two carbon atoms, using threshold photoelectron-photoion coincidence (TPEPICO) spectroscopy and synchrotron radiation as a tunable VUV photoionisation source. To date, we have studied saturated and unsaturated perfluorocarbons, C_xF_y^+ ,^{8,9} and three HFCs; pentafluoroethane,¹⁰ and the two isomers of tetrafluoroethane.¹¹ In this paper we report data for the two isomers of the trifluoroethane cation; $\text{CF}_3\text{-CH}_3^+$ (R143a, labelled 1,1,1 in this paper) and $\text{CHF}_2\text{-CH}_2\text{F}^+$ (R143 and labelled 1,1,2 here). Preliminary results for the 1,1,1 isomer have been reported elsewhere.¹² Research carried out on these two isomers of trifluoroethane to date has focussed on the structure, conformational stability, and spectroscopy of the neutral molecule. These investigations include infrared and Raman studies,¹³ electron diffraction,¹⁴ and *ab initio* calculations.^{15–19}

[†] Electronic supplementary information (ESI) available: Figs. 1–7 in colour. See <http://www.rsc.org/suppdata/cp/b4/b404604h/>

[‡] Present address: Department of Chemistry, University of California Riverside, CA 92521-0403, USA.

[§] Present address: Department of Physics, University of Windsor, Ontario, Canada N9B 3P4.

A microwave spectrum has been reported only for the 1,1,1 isomer,²⁰ and recommended values for the structure, vibrational frequencies and standard enthalpy of formation for this isomer have been published.²¹ The only papers describing properties of the ionised trifluoroethanes report He I photoelectron and electron-impact mass spectrometric studies of the 1,1,1 isomer.^{22,23} In the latter paper, appearance energies of the fragment ions were measured.²³ To our knowledge, there are no equivalent data for the 1,1,2 isomer.

In this paper we describe the results of a TPEPICO study of $\text{CF}_3\text{-CH}_3$ and $\text{CHF}_2\text{-CH}_2\text{F}$ from the onset of ionisation (*ca.* 12 eV) up to 24 eV. The threshold photoelectron spectrum (TPES) and state-selected fragmentation studies of the parent ions are presented. Breakdown diagrams, yielding the formation probability of fragment ions as a function of photon energy, are obtained. The mean translational kinetic energy releases for unimolecular fragmentation proceeding *via* a single-bond cleavage are determined, and compared with the predictions of statistical and dynamical impulsive models. Enthalpies of formation at 298 K for the two neutral isomers and some fragment ions are also determined. These experimental results are complemented and compared with *ab initio* calculations of the structure of the two isomers of trifluoroethane, their ionisation energies, and the enthalpy of formation of several fragment ions.

2. Theoretical and experimental methods

2.1 Computational methods

Using Gaussian 98, *ab initio* molecular orbital calculations have been performed for $\text{CF}_3\text{-CH}_3$ and $\text{CHF}_2\text{-CH}_2\text{F}$, both in their neutral ground states and in the ground states of the parent cations. Calculations have also been performed for fragments produced by VUV dissociative photoionisation (*e.g.* $\text{CF}_2\text{-CH}_3^+$). Structures for all species were optimised using the second-order Møller–Plesset theory (MP2) with the 6-31G(d) basis set, and all electrons were included at the MP2(full)/6-31G(d) level. The MP2(full)/6-31G(d) structures were then employed for energy calculations according to the Gaussian-2 (G2) procedure.²⁴ This procedure involves single-point total energy calculations at the MP4/6-311G(d,p), QCISD(T)/6-311g(d,p), MP4/6-311G(d,p), MP4/6-311G(2df,p), and MP2/6-311G(3df,2p) levels. A small empirical correction is employed to include the high-level correlation effects in the calculations of the total electronic energies (EE). The HF/6-31G(d) harmonic vibrational frequencies, scaled by 0.8929, are applied for zero-point vibrational energy (ZPVE) corrections to obtain the total energies at 0 K ($E_0 = \text{EE} + \text{ZPVE}$). The enthalpies of formation at 298 K ($\Delta_f H^\circ_{298}$) for molecular species are calculated using total energies and the scaled HF/6-31G(d) harmonic frequencies, leading to predicted enthalpies of unimolecular reactions (*e.g.* $\text{CHF}_2\text{-CH}_2\text{F} \rightarrow \text{CHF-CH}_2\text{F}^+ + \text{F} + \text{e}^-$). The agreement between G2 and experimental results is usually well within ± 0.2 eV (or ± 20 kJ mol⁻¹).²⁴

2.2 Experimental methods

The TPEPICO apparatus has been described in detail elsewhere.^{11,25} Synchrotron radiation from the 2 GeV electron storage ring at the Daresbury Laboratory is energy-selected using a 1 m Seya monochromator equipped with two gratings, covering the energy range *ca.* 8–40 eV. The majority of the experiments for $\text{CF}_3\text{-CH}_3$ were performed using the higher-energy grating (range 105–30 nm (12–40 eV), blazed at *ca.* 55 nm) with an optical resolution of 0.3 nm; this corresponds to an energy resolution of 0.035 and 0.140 eV at 12 and 24 eV, respectively. For $\text{CHF}_2\text{-CH}_2\text{F}$, most experiments used the lower-energy grating (range 150–60 nm (8–21 eV), blazed at *ca.* 90 nm) with the same resolution. With the higher-energy

grating, the effects of second-order radiation are insignificant for $\lambda < 95$ nm, and for the lower-energy grating insignificant for $\lambda < 120$ nm.

The VUV radiation is admitted into the interaction region through a glass capillary, and the photon flux is monitored using a photomultiplier tube *via* the visible fluorescence from a sodium salicylate-coated window. Threshold photoelectrons and fragment cations produced by photoionisation are extracted in opposite directions by a 20 V cm⁻¹ electric field applied across the interaction region, and detected by a single channel electron multiplier and microchannel plates, respectively. The design of threshold electron analyser and time-of-flight mass spectrometer are described elsewhere.^{11,25} Following discrimination and pulse shaping, signals from the electron and ion detectors pass to a time-to-digital converter (TDC) configured in the multi-hit mode and mounted in a PC. The electrons provide the ‘start’, the ions the ‘stop’ pulses, allowing signals from the same ionisation process to be detected in delayed coincidence.

TPEPICO spectra are recorded either continuously as a function of photon energy or at a fixed energy. In the scanning-energy mode, flux-normalized TPEPICO spectra are recorded as three-dimensional, false-colour maps of coincidence count *vs.* ion flight time *vs.* photon energy. A cut through the map at a fixed photon energy yields the time of flight mass spectrum (TOF-MS), which identifies the fragment ions formed in the dissociative photoionisation at that energy. Alternatively, a background-subtracted cut taken through the histogram at a fixed flight time, corresponding to a mass peak in the TOF-MS, gives an ion yield curve. In this mode of operation, the TOF resolution is degraded to 64 ns so that *all* the fragment ions are observed simultaneously. The threshold electron and total ion counts are also recorded, yielding the TPES and total ion yield curve, respectively. In the fixed-energy mode, time-of-flight spectra (later referred to as TPEPICO-TOF spectra) are measured at *single* energies corresponding to peaks in the TPES. Now a TOF resolution as high as the signal level permits is employed, typically 8 ns, and usually only one fragment ion is observed per spectrum. Fragment ions often have enough translational energy for the peaks comprising the TPEPICO-TOF spectra to be substantially broadened. From an analysis of the peak shape, it is then possible to obtain kinetic energy release distributions (KERDs) and hence mean kinetic energy releases, $\langle \text{KE} \rangle_T$.^{26,27}

The sample gases, $\text{CF}_3\text{-CH}_3$ and $\text{CHF}_2\text{-CH}_2\text{F}$, were obtained commercially (Fluorochem Ltd., UK), with a stated purity of >99% and used without further purification. The operating pressure was *ca.* 5×10^{-5} mbar, with a chamber base pressure of *ca.* 5×10^{-8} mbar.

3. Energetics of the dissociation channels

The energetics of the dissociation channels of $\text{CF}_3\text{-CH}_3^+$ and $\text{CHF}_2\text{-CH}_2\text{F}^+$ into fragment ions are given in Table 1. The enthalpies of reaction at temperature T , $\Delta_r H^\circ_T$, associated with the unimolecular reaction $\text{AB} \rightarrow \text{A}^+ + \text{B} + \text{e}^-$, where AB refers to the parent molecule, are determined by calculating the difference between the enthalpies of formation of products and reactants. We have used $\Delta_f H^\circ$ data at 298 K for neutrals taken from the Janaf tables,²⁸ for ions from Lias *et al.*,²⁹ and these values, in units of kJ mol⁻¹, are shown in brackets in column 1 of the table. Where values different from these compilations are used, they are referenced later. The values used for the two parent molecules, -751 ± 10 kJ mol⁻¹ for $\text{CF}_3\text{-CH}_3$ and -671 ± 12 kJ mol⁻¹ for $\text{CHF}_2\text{-CH}_2\text{F}$, are discussed in Section 5.

Our experiment measures appearance energies at 298 K (AE_{298}) of fragment ions, and some discussion is pertinent on how these data are measured and how they relate to $\Delta_f H^\circ_{298}$. Columns 2 and 3 of Table 1 give AE_{298} and $\Delta_f H^\circ_{298}$ values for the *major* fragment ions; a major ion is defined as one produced

Table 1 Energetics of dissociative photoionisation pathways of CF₃-CH₃ and CHF₂-CH₂F

| | AE ₂₉₈ /eV | Δ _r H° ₂₉₈ /eV ^d | G2/eV ^e |
|---|-----------------------|---|--------------------|
| Major ^a ion products of CF ₃ -CH ₃ (-751) ^c | | | |
| CF ₃ -CH ₃ ⁺ + e ⁻ | 12.98 (4) | | 12.54 |
| CF ₃ ⁺ (+406) + CH ₃ (+146) + e ⁻ | 13.25 (5) | 13.41 (5) | 13.52 |
| CH ₃ ⁺ (+1095) + CF ₃ (-466) + e ⁻ | 14.25 (5) | 14.41 (5) | 14.28 |
| CF ₂ -CH ₃ ⁺ (unknown) ^f + F (+79) + e ⁻ | 14.10 (5) | 14.26 (7) | 13.40 |
| Minor ^b ion products of CF ₃ -CH ₃ (-751) | | | |
| CF-CH ₂ ⁺ (+951) + F ₂ (0) + H (+218) + e ⁻ | 17.1 (1) | 15.59 | |
| CF-CH ₂ ⁺ (+951) + HF (-277) + F (79) + e ⁻ | | 19.90 | |
| CF-CH ₂ ⁺ (+951) + 2F (+158) + H (+218) + e ⁻ | | 21.54 | |
| CF ₂ -CH ₂ ⁺ (648) + HF (-277) + e ⁻ | >19.5 (5) | 11.63 | |
| CF ₂ -CH ₂ ⁺ (648) + H (+218) + F (+79) + e ⁻ | | 17.58 | |
| CH ₂ F ⁺ (+833) + CHF ₂ (-237) + e ⁻ | 16.5 (5) | 13.96 | |
| CH ₂ F ⁺ (+833) + CF (+255) + HF (-277) + e ⁻ | | 16.19 | |
| CH ₂ F ⁺ (+833) + CF ₂ (-182) + H (+218) + e ⁻ | | 16.79 | |
| Major ^a ion products of CHF ₂ -CH ₂ F (-671) | | | |
| CHF ₂ -CH ₂ F ⁺ + e ⁻ | 11.88 (4) | | 11.68 |
| CHF ₂ ⁺ (+604) + CH ₂ F (-33) + e ⁻ | 12.50 (4) | 12.65 (4) | 12.76 |
| CH ₂ F ⁺ (+833) + CHF ₂ (-237) + e ⁻ | 13.19 (4) | 13.34 (4) | 13.08 |
| CHF-CH ₂ F ⁺ (unknown) ^g + F (+79) + e ⁻ | 14.51 (5) | 14.65 (5) | 13.72 |
| CHF ₂ -CH ₂ ⁺ (unknown) + F (+79) + e ⁻ | | | 12.42 |
| Minor ^b ion products of CHF ₂ -CH ₂ F (-671) | | | |
| CF-CH ₂ ⁺ (+951) + HF (-277) + F (79) + e ⁻ | 16.21 (5) | 14.76 | |
| CF-CH ₂ ⁺ (+951) + F ₂ (0) + H (+218) + e ⁻ | | 19.07 | |
| CF-CH ₂ ⁺ (+951) + 2F (+158) + H (+218) + e ⁻ | | 20.71 | |

^a Major ion product is defined as either the parent ion, or a fragment ion caused by a single bond fission. ^b Minor ion product is defined as a fragment ion caused by fission of multiple bonds. ^c Literature values for Δ_rH°₂₉₈, given in brackets in Column 1, have units of kJ mol⁻¹ (Section 3). ^d For the major ions, the value of Δ_rH°₂₉₈ is derived from AE₂₉₈ of the fragment ion using the procedure of Traeger and McLoughlin.³⁰ For the minor ions, the value of Δ_rH°₂₉₈ is given by the enthalpy of formation of products minus that of reactants; we use values for Δ_rH°₂₉₈ given in brackets in Column 1, where the units are kJ mol⁻¹. ^e Enthalpy of reaction at 298 K, using enthalpies of formation of products and reactants calculated at the G2 level of theory with optimised minimum-energy geometries. ^f Our data yields an upper limit for Δ_rH°₂₉₈(CF₂-CH₃⁺) of 546 ± 11 kJ mol⁻¹. ^g Our data yields an upper limit for Δ_rH°₂₉₈(CHF-CH₂F⁺) of 663 ± 13 kJ mol⁻¹.

by a single bond fission. The AE₂₉₈ of each fragment ion has been determined from the extrapolation of the linear portion of the ion yield to zero signal. At the optical resolution of our experiment, this is equivalent to the first onset of signal. No corrections have been made for exit channel barriers or kinetic shifts, and AEs determined in this way can only be regarded as upper limits. The procedure of Traeger and McLoughlin³⁰ has been used to convert the AE₂₉₈ into Δ_rH°₂₉₈. For the reaction AB → A⁺ + B + e⁻, Traeger and McLoughlin have shown that:

$$\Delta_r H_{298}^{\circ} \leq AE(A^+)_{298} + \int_0^{298} c_p(A^+)dT + \int_0^{298} c_p(B)dT - \frac{5RT}{2} \quad (1)$$

As above, the upper limit for Δ_rH°₂₉₈ arises due to the fact that there may be an exit channel barrier and/or a kinetic shift; if both are zero, then the equality sign in eqn. (1) applies. This equation assumes the validity of the stationary electron convention that, at threshold, the electron has zero translational energy. If the last three terms in eqn. (1) are ignored, a significant error may be introduced in equating the measured AE₂₉₈ into an upper limit for Δ_rH°₂₉₈. The second and third terms on the right-hand side of eqn. (1), equivalent to H°₂₉₈ - H°₀ for A⁺ or B, contain contributions from translational (2.5RT), rotational (1.5RT) and vibrational (N_Ahν/[exp(hν/k_BT) - 1] per vibrational mode) motion, evaluated at

T = 298 K. The error is greater the larger the number of vibrational modes, and hence the number of atoms in A⁺ and B. Vibrational frequencies of A⁺ and B are taken from standard sources.^{28,31} If they are not available, they are estimated by comparison with isoelectronic molecules.

For the *minor* fragment ions, defined as ions caused by a fission of multiple bonds, column 3 of Table 1 gives the values of Δ_rH°₂₉₈ calculated from the enthalpy of formation of products minus that of reactants, using the values in column 1. Column 2 shows the AE₂₉₈ of the minor ion, and we have not converted this value into an upper limit for Δ_rH°₂₉₈ via the procedure of Traeger and McLoughlin. Comparison of the values in Columns 2 and 3 can suggest what neutral partner(s) form with the minor fragment ion.

4. Theoretical results

4.1 Structure of CF₃-CH₃ and CF₃-CH₃⁺, and orbital character

The optimised geometries of CF₃-CH₃ and CF₃-CH₃⁺ (Table 2) have been obtained at the MP2(full)/6-31G(d) level. Both have a staggered C_{3v} symmetry, and the geometry for the neutral is very close to that from electron diffraction¹⁴ and microwave²⁰ studies. The highest occupied molecular orbital (HOMO) has mainly C-C σ character (Fig. 1). Loss of an electron from this orbital yields the ground state of CF₃-CH₃⁺ which is predicted to have a lengthened C-C bond. The orbitals of next lowest energy (labelled HOMO - 1(a) and HOMO - 1(b) in Fig. 1) are degenerate π orbitals with a node on different C-C-H planes. They are largely localised on the CH₃ group

Table 2 Optimised minimum-energy geometries^a for the ground electronic state of neutral and parent cation of 1,1,1 trifluoroethane calculated at the MP2(full)/6-31G(d) level of theory

| | CF ₃ -CH ₃ | CF ₃ -CH ₃ ⁺ |
|--------------------------------|----------------------------------|---|
| Symmetry | C _{3v} | C _{3v} |
| Electronic state | ¹ A ₁ | ² A ₁ |
| R(C1,C2) | 1.495 | 1.922 |
| R(C1,Fn) | 1.353 | 1.287 |
| R(C2,Hn) | 1.090 | 1.088 |
| θ(C2,C1,Fn) | 111.6 | 101.8 |
| θ(C1,C2,Hn) | 109.2 | 98.8 |
| θ(Fm,C1,Fn) | 107.2 | 115.9 |
| θ(Hm,C2,Hn) | 109.7 | 117.7 |
| D(Fm,C1,C2,Hn) | 180.0, +60.0 or -60.0 | 180.0, +60.0 or -60.0 |
| E ₀ /E _h | -377.133224 | -376.673470 |
| Adiabatic IE ₀ /eV | 12.51 | |

^a Bond lengths, *R*, in Å; bond angles, *θ* and dihedral angles, *D*, in degrees.

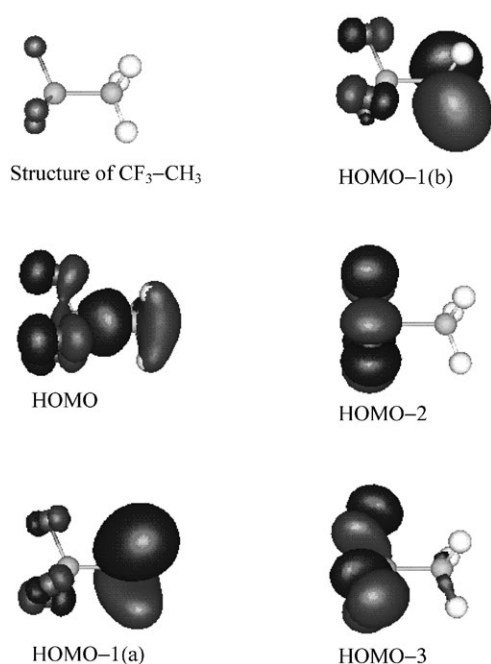


Fig. 1 Computed minimum energy structure of the ground state of CF₃-CH₃ and its five highest valence molecular orbitals. The orbitals are calculated at the MP2/6-31(d) level of theory.

with some C-H bonding character, and give rise to two bands due to Jahn-Teller splitting following ionisation. The next two orbitals, labelled HOMO - 2 and HOMO - 3, are mainly F 2pπ nonbonding in character. We note that ionisation from these orbitals will give rise to excited states of CF₃-CH₃⁺ which are expected to dissociate *via* F-loss to CF₂-CH₃⁺ + F, provided dissociation follows a rapid impulsive mechanism.

At this level of theory, the main geometry changes upon ionisation from the HOMO of CF₃-CH₃ are a C-C bond length increase of 0.42 Å, a C-F bond length decrease of 0.06 Å, and a transition from non-planar to planar geometry for the CF₃ and CH₃ groups where the positive charge is localised. G2 energies are computed for the ground states of CF₃-CH₃ and CF₃-CH₃⁺. From the difference, an adiabatic ionisation energy (AIE) of 12.51 eV at 0 K, 12.54 eV at 298 K, is obtained. The unfavourable Franck-Condon factors at the onset of the first photoelectron band will almost certainly lead to an experimental onset of signal which is significantly greater than this *ab initio* value. A vertical ionisation energy (VIE) of 13.92 eV was deduced from the ground state of CF₃-CH₃, using the G2 energy for CF₃-CH₃⁺ calculated with its geometry constrained to that of CF₃-CH₃.

4.2 Structure of CHF₂-CH₂F and CHF₂-CH₂F⁺, and orbital character

The minimum energy geometries of CHF₂-CH₂F and CHF₂-CH₂F⁺ have also been determined at the MP2(full)/6-31G(d) level (Table 3). For the neutral, the trans structure with a symmetry of C₁ is more stable, in agreement with the conclusions reported through analysis of infrared/Raman spectra and electron diffraction.^{13,14} For CHF₂-CH₂F⁺, the main structural change after ionisation is an increase of 0.43 Å in the C-C bond length, a decrease of 0.07 Å in the C-F bond length, and an increase in the ∠FCF, ∠FCH and ∠HCH bond angles in both the CHF₂ and CH₂F groups. Thus, both the CHF₂ and CH₂F groups adopt a more planar structure upon ionisation. There is also a small rotation about the C-C bond upon ionisation that leads to four atoms FCCF being approximately located in a plane. The AIE of CHF₂-CH₂F was calculated through the G2 energy difference between the ground state of the neutral molecule and its cation. A value of 11.68 eV is then deduced at 298 K. As with CF₃-CH₃, the poor Franck-Condon factor in the threshold region will almost certainly lead to an overestimation of the adiabatic ionisation energy from the onset of signal in the threshold photoelectron spectrum compared to this *ab initio* value. The VIE of CHF₂-CH₂F was not determined.

The structure of the neutral molecule and the five highest valence molecular orbitals (MOs) are shown in Fig 2. At this level of theory, the HOMO consists of mainly C-C σ bonding and C-H σ* antibonding character, consistent with the changes in geometry after ionisation. The orbital of next highest energy (*i.e.* HOMO - 1) is a π* orbital localized on the CH₂F group, with C-H σ bonding character. The (HOMO - 2) orbital is a hybrid orbital largely localized on the CHF₂ group, consisting of C-H σ bonding and F 2pπ lone-pair character. Both of the next two higher excited valence orbitals (HOMO - 3 and HOMO - 4) are mainly composed of F 2pπ lone-pair nonbonding orbitals. The removal of an electron from this type of orbital is expected to result in C-F bond fission, *i.e.* fragmentation to C₂H₃F₂⁺ + F, provided the dissociation follows an impulsive mechanism. Note that if this mechanism is operative, the electron density maps of the orbitals (Fig. 2) suggest that F loss from the (HOMO - 3) orbital should produce predominantly the isomer CHF-CH₂F⁺, whereas F loss from (HOMO - 4) will yield both CHF-CH₂F⁺ and CHF₂-CH₂⁺.

4.3 Calculation of Δ_rH^o₂₉₈ for dissociative photoionisation reactions

As described earlier, the enthalpies of formation at 298 K of both isomers of C₂F₃H₃ and all the neutral and fragment ions

Table 3 Optimised minimum-energy geometries^a for the ground electronic state of neutral and parent cation of 1,1,2 trifluoroethane calculated at the MP2(full)/6-31G(d) level of theory

| | CHF ₂ -CH ₂ F | CHF ₂ -CH ₂ F ⁺ |
|--------------------------------|-------------------------------------|--|
| Symmetry | C ₁ | C ₁ |
| Electronic state | ¹ A' | ² A' |
| R(C-C) | 1.505 | 1.921 |
| CHF ₂ group | | |
| R(C-H) | 1.092 | 1.095 |
| R(C-F) | 1.371 | 1.293 |
| | 1.364 | 1.290 |
| θ(FCF) | 108.3 | 114.8 |
| θ(FCH) | 109.1 | 117.3 |
| | 108.5 | 116.8 |
| CH ₂ F group | | |
| R(C-F) | 1.388 | 1.303 |
| R(C-H) | 1.092 | 1.091 |
| | 1.092 | 1.090 |
| θ(HCH) | 109.7 | 114.8 |
| θ(FCH) | 109.4 | 115.0 |
| | 110.2 | 121.5 |
| D(FCCF) | 176.0 | 179.7 |
| E ₀ /E _h | -377.098895 | -376.670595 |
| Adiabatic IE ₀ /eV | 11.65 | |

^a Bond lengths, R, in Å; bond angles, θ and dihedral angles, D, in degrees.

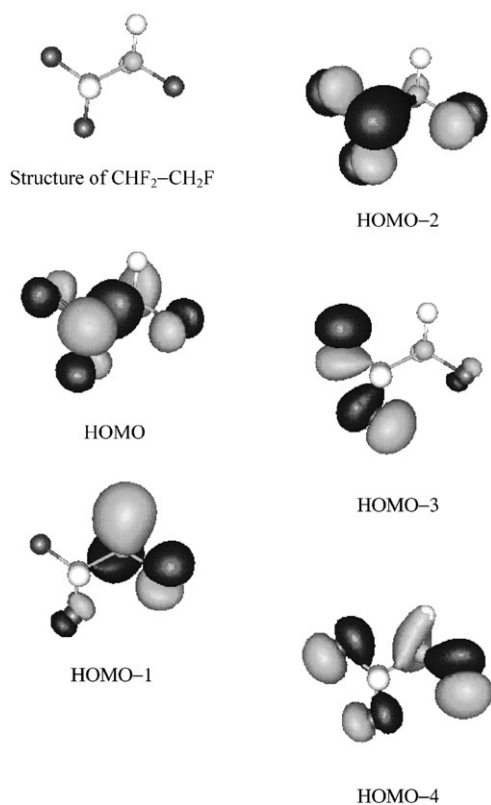


Fig. 2 Computed minimum energy structure of the ground state of CHF₂-CH₂F and its five highest valence molecular orbitals. The orbitals are calculated at the MP2/6-31(d) level of theory.

observed by dissociative photoionisation have been calculated. It is therefore possible to calculate the enthalpy of reaction at this temperature for all the observed reactions. For reactions involving production of a major fragment ion, these values are shown in column 4 of Table 1, and we should note that these G2 calculations refer specifically to reactants and products whose energies have been determined with optimised geometries.

5. Experimental results and discussion

5.1 Threshold photoelectron spectra of CF₃-CH₃ and CHF₂-CH₂F

The threshold photoelectron spectrum (TPES) of CF₃-CH₃ was measured in the range 13–22 eV at an optical resolution of 0.3 nm (Fig 3). The vertical ionisation energies of the six peaks, labelled as the \tilde{X} , \tilde{A} , \tilde{B} , \tilde{C} , \tilde{D} and \tilde{E} states of the parent ion, are 14.56, 15.19, 16.03, 16.91, 19.00 and 20.23 eV, respectively. The onset of ionisation is 12.98 ± 0.04 eV. A notable feature of this spectrum is that the ground electronic state of CF₃-CH₃⁺ partially overlaps that of the first excited state. This observation is different from CHF₂-CF₃, CF₃-CH₂F and CHF₂-CHF₂, and CHF₂-CH₃,^{10–12} where these molecules all have broad but well-separated first photoelectron bands following electron removal from the HOMO. These four molecules also show an increase in the energy of the onset of ionisation as the number of fluorine atoms increases, an effect already noted by Sauvageau *et al.*²² from He I photoelectron spectra. Furthermore, corresponding bands of higher energy in their TPES shift to higher energy with an increase in the number of fluorine atoms. These observations are consistent with the perfluoro effect, arising from the higher effective nuclear charge of a fluorine compared to a hydrogen atom and the corresponding stabilisation of the σ orbitals in fluorinated ethanes.³²

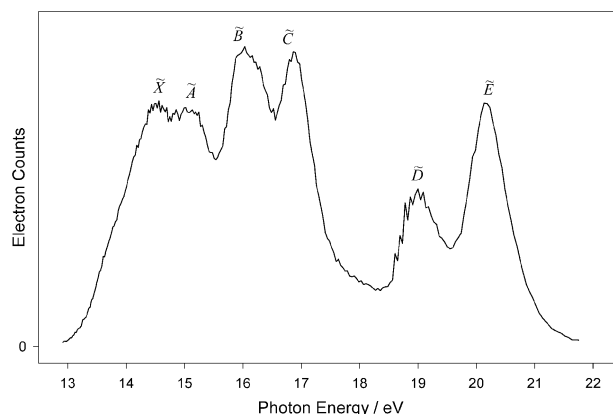


Fig. 3 Threshold photoelectron spectrum of CF₃-CH₃. The optical resolution is 0.3 nm.

The anomalous behaviour of $\text{CF}_3\text{-CH}_3$, with its unusually high onset of ionisation giving rise to overlap of the first and second photoelectron bands, may arise due to the higher symmetry of this molecule, although the same behaviour is observed for $\text{CHF}_2\text{-CH}_2\text{F}$ which has lower symmetry (see later). Note that the *ab initio* calculations described in Section 4 show that the energy difference between the HOMO of $\text{CF}_3\text{-CH}_3$ and the degenerate π orbitals is small, only 0.6 eV at the MP2/6-31G(d) level. As with all the other hydrofluorocarbons, electron removal from the strong C–C σ -bonding HOMO will yield a broad photoelectron band. Thus, the overlap of the first and second photoelectron bands in the (T)PES of $\text{CF}_3\text{-CH}_3$ is not surprising. The two bands centred around 16 and 17 eV in the TPES of $\text{CF}_3\text{-CH}_3$ are likely to be due to removal of an electron from the (HOMO – 2) and (HOMO – 3) molecular orbitals of F $2p\pi$ lone pair character.

The band positions reported by Sauvageau *et al.*²² from the He I photoelectron spectrum of $\text{CF}_3\text{-CH}_3$ are similar to those of the TPES reported here, but the relative intensities of the bands are different. This difference could be due either to a change in the relative ionisation cross section between excitation at threshold and excitation above threshold with non-resonant radiation, or to autoionisation effects. As noted in our previous papers on small perfluorocarbons,^{8,9} a comparison of the total ion yield and the integrated TPES can reveal the peaks in the TPES that arise *via* autoionisation. There is excellent agreement between the integrated TPES and the total ion yield of $\text{CF}_3\text{-CH}_3$,³³ indicating that no autoionisation processes occur in this energy area. It is likely, therefore, that for $\text{CF}_3\text{-CH}_3$ the former explanation is correct.

The onset of ionisation, 12.98 ± 0.04 eV, is 0.28 eV lower than that reported by electron impact ionisation,²³ but 0.44 eV higher than the *ab initio* calculation at 298 K (Section 4.1). This latter difference must be due to the near-zero Franck–Condon factor at the onset of the first photoelectron band due to the large geometry change upon ionisation. Combining the experimental onset with the value for $\Delta_f H^\circ_{298}(\text{CF}_3\text{-CH}_3)$ of -751 ± 10 kJ mol⁻¹ (see later), we determine $\Delta_f H^\circ_{298}(\text{CF}_3\text{-CH}_3^+) < 501 \pm 11$ kJ mol⁻¹.

The threshold photoelectron spectrum of $\text{CHF}_2\text{-CH}_2\text{F}$ was also measured with an optical resolution of 0.3 nm (Fig 4). The vertical ionisation energies of the eight observed peaks (or shoulders) in the range 12–25 eV are determined to be 13.03, 13.75, 14.96, 15.97, 17.51, 18.62, 19.17 and 22.26 eV, and these are labelled as ionisation to the \tilde{X} , \tilde{A} , \tilde{B} , \tilde{C} , \tilde{D} , \tilde{E} , \tilde{F} and \tilde{G} states of the parent ion. The band corresponding to the ground ionic state is relatively weak and broad, consistent with the large change in geometry following electron removal from the HOMO of C–C σ -bonding character. The next two bands, labelled \tilde{A} and \tilde{B} at 13.75 and 14.96 eV respectively, are assigned to mainly C–H σ -bonding orbitals localised on the

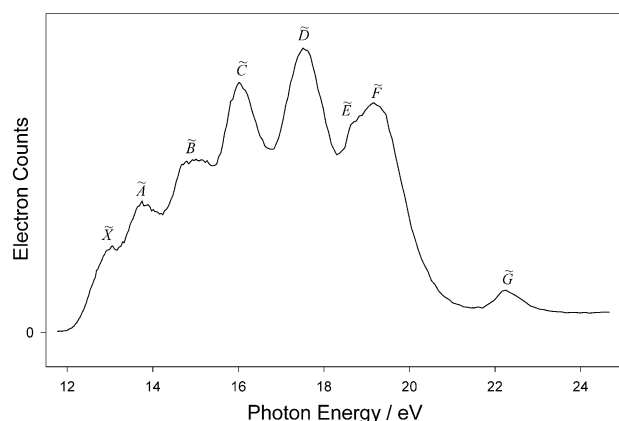


Fig. 4 Threshold photoelectron spectrum of $\text{CHF}_2\text{-CH}_2\text{F}$. The optical resolution is 0.3 nm.

CH_2F and CHF_2 groups, respectively. Note that, as with $\text{CF}_3\text{-CH}_3$, the \tilde{X} and \tilde{A} bands are not well separated. At higher energy the TPES of $\text{CHF}_2\text{-CH}_2\text{F}$ shows two relatively narrow peaks centred at 15.97 and 17.51 eV, labelled \tilde{C} and \tilde{D} . Narrow peaks in photoelectron spectra with unresolved vibrational structure often relate to the removal of a non-bonding electron, confirming that the (HOMO – 3) and (HOMO – 4) molecular orbitals of this molecule are essentially F $2p\pi$ nonbonding in character. It is shown later that 15.97 eV corresponds to the photon energy leading to the maximum intensity of the fragment ion $\text{CHF-CH}_2\text{F}^+$ produced by breaking a C–F bond. This phenomenon of isolated state-selected behaviour in the hydrofluorocarbon cations is relatively common, and has been observed by us and others in $\text{C}_2\text{F}_4\text{H}_2^+$, $\text{C}_2\text{F}_5\text{H}^+$ and C_2F_6^+ .^{10,11,34}

The observed onset of signal in the TPES occurs at 11.88 ± 0.04 eV. This experimental ionisation threshold is 0.20 eV higher than the calculated AIE of $\text{CHF}_2\text{-CH}_2\text{F}$ from the G2 calculation. This difference is due to the very low Franck–Condon factor in the threshold region, and the observed ionisation threshold should only be regarded as an upper limit. Combining the observed IE with a value for $\Delta_f H^\circ_{298}(\text{CHF}_2\text{-CH}_2\text{F})$ of -671 ± 12 kJ mol⁻¹ (see later), we determine $\Delta_f H^\circ_{298}(\text{CHF}_2\text{-CH}_2\text{F}^+) < 475 \pm 13$ kJ mol⁻¹. As with $\text{CF}_3\text{-CH}_3$, the excellent agreement between the integrated TPES and the total ion yield suggests that autoionisation is not an important process in this energy range.³³ We note no published HeI photoelectron spectrum exists to compare the relative peak intensities to the spectrum recorded under threshold conditions (Fig. 4).

5.2 Scanning-energy TPEPICO spectra

5.2.1 Coincidence ion yields of $\text{CF}_3\text{-CH}_3^+$. A TPEPICO spectrum in the scanning-energy mode was recorded for $\text{CF}_3\text{-CH}_3$ from 12–22 eV at a wavelength resolution of 0.3 nm and an ion TOF resolution of 64 ns. The parent ion and the fragments CF_3^+ , CH_3^+ , $\text{CF}_2\text{-CH}_3^+$ and CF-CH_2^+ were detected as the strongest five ions, and their yields are shown in Fig. 5. The parent ion appears weakly at the lowest energy, then with increasing energy the three major fragment ions CF_3^+ , $\text{CF}_2\text{-CH}_3^+$ and CH_3^+ are observed. These four ions are the main fragments within the energy range 12–17 eV. At higher energy, an ion of mass 45 u, almost certainly CF-CH_2^+ , appears gradually and becomes the dominant fragment in the range 18–21 eV. Very weak minor fragment ions are also observed with masses of 33 u (CH_2F^+) and 64 u ($\text{CF}_2\text{-CH}_2^+$), but their yields are not shown in Fig. 5. We comment that as with $\text{CHF}_2\text{-CF}_3^+$,¹⁰ but unlike both isomers of $\text{C}_2\text{H}_2\text{F}_4^+$,¹¹ we did not observe any signal due to $\text{CF}_3\text{-CH}_2^+$,

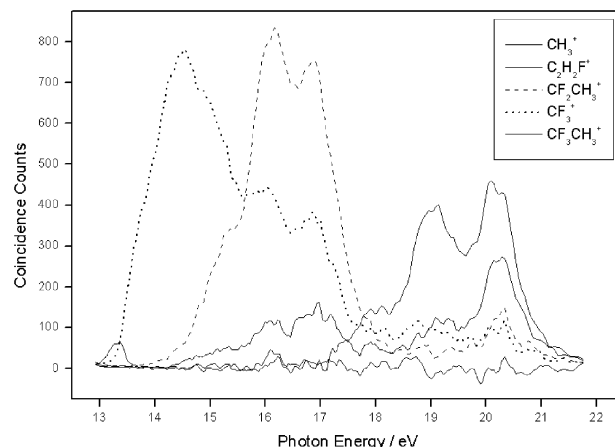


Fig. 5 Coincidence ion yields from $\text{CF}_3\text{-CH}_3$ over the energy range 13–22 eV. The optical resolution is 0.3 nm.

corresponding to C–H bond fission. Note that by using a TOF resolution of only 64 ns, a definitive determination of the number of hydrogen atoms in a fragment ion can be problematic, but we are confident of these assignments.

Within the energy range of the ground ionic state, the cation $\text{CF}_3\text{-CH}_3^+$ is observed with an appearance energy of 12.98 ± 0.04 eV. This signal is relatively weak and appears over a narrow energy range, suggesting that the $\tilde{\text{X}}$ state of $\text{CF}_3\text{-CH}_3^+$ is bound only for a small range of low vibrational levels in the Franck–Condon envelope. The slow rise of the ion yield in the threshold region is due to the small Franck–Condon factor at threshold. Electron impact studies have observed an ionisation threshold of 13.26 eV.²³ Due to the electron energy resolution being significantly inferior, the results from our photon-impact experiment should be more accurate.

The CF_3^+ fragment ion has an AE_{298} of 13.25 ± 0.05 eV. This fragment is the most intense and dominates until 15.5 eV. Using the procedure of Traeger and McLoughlin,³⁰ this value of AE_{298} converts into an upper limit of 13.41 ± 0.05 eV for $\Delta_f H^\circ_{298}$ for the reaction $\text{CF}_3\text{-CH}_3 \rightarrow \text{CF}_3^+ + \text{CH}_3 + \text{e}^-$ (Table 1). C–C bond cleavage can also produce CH_3^+ as the fragment ion, where we measure AE_{298} to be 14.25 ± 0.05 eV. As above, this value can be used to determine an upper limit of $\Delta_f H^\circ_{298}$ for the reaction $\text{CF}_3\text{-CH}_3 \rightarrow \text{CH}_3^+ + \text{CF}_3 + \text{e}^-$ to be 14.41 ± 0.05 eV (Table 1). G2 calculations predict $\Delta_f H^\circ_{298}$ for these two reactions to be very similar, 13.52 and 14.28 eV, respectively. Our experimental values can be used to determine an average $\Delta_f H^\circ_{298}$ for the parent neutral molecule. Using literature values of $\Delta_f H^\circ_{298}$ for CH_3 ,²⁸ CH_3^+ ,³⁵ CF_3 ,³⁶ and CF_3^+ ,³⁷ a lower limit of -751 ± 10 kJ mol⁻¹ is determined for $\Delta_f H^\circ_{298}(\text{CF}_3\text{-CH}_3)$. This value is in excellent agreement with -771 kJ mol⁻¹ from our G2 calculation, and independent theoretical values of -746 ± 2 and -755 from Chen *et al.*²¹ and Zachariah *et al.*¹⁸ By assuming that there are no exit channel barriers or kinetic shifts in either reaction we equate our lower limit value with the absolute value. Henceforth, therefore, we use $\Delta_f H^\circ_{298}(\text{CF}_3\text{-CH}_3) = -751 \pm 10$ kJ mol⁻¹.

The $\text{CF}_2\text{-CH}_3^+$ fragment ion signal appears with a threshold of $14.10 \text{ eV} \pm 0.05$ eV, corresponding to an upper limit of $\Delta_f H^\circ_{298}$ for the reaction $\text{CF}_3\text{-CH}_3 \rightarrow \text{CF}_2\text{-CH}_3^+ + \text{F} + \text{e}^-$ of 14.26 eV. The signal increases slowly, then rises rapidly from approximately 15.5 eV. From 14.1–17.8 eV, the peaks in the ion yield of $\text{CF}_2\text{-CH}_3^+$ match the bands in the TPES. An interesting point is that the emergence of the second threshold at 15.5 eV corresponds to the onset of the $\tilde{\text{B}}$ -state band in the TPES. The *ab initio* calculation shows that this band is associated with the electronic state caused largely by electron loss from the (HOMO – 2) F 2p π nonbonding orbital. The (HOMO – 3) orbital also has F 2p π nonbonding character. The similarity of the ion signal with the shape of the $\tilde{\text{B}}$ and $\tilde{\text{C}}$ bands in the TPES suggest that $\text{CF}_2\text{-CH}_3^+$ is produced directly *via* C–F bond cleavage by an impulsive mechanism from these electronics states of the parent cation without prior internal energy conversion to the ground state. From the upper limit of $\Delta_f H^\circ_{298}$, we determine $\Delta_f H^\circ_{298}(\text{CF}_2\text{-CH}_3^+) \leq 546 \pm 11$ kJ mol⁻¹. We were not able to measure the kinetic energy release in the dissociation $\text{CF}_3\text{-CH}_3^+ \rightarrow \text{CF}_2\text{-CH}_3^+ + \text{F}$ (Section 6), but by analogy with the 1,1,2 isomer we can assume that it may be considerable. It is likely, therefore, that the true enthalpy of formation of this ion is significantly lower than this value. A G2 calculation, for instance, predicts $\Delta_f H^\circ_{298}(\text{CF}_2\text{-CH}_3^+)$ to be 443 kJ mol⁻¹, and Lias *et al.*²⁹ give an indirect value of 458 kJ mol⁻¹. These data are therefore self-consistent, and suggest that the $\text{AE}_{298}(\text{CF}_2\text{-CH}_3^+)$ lies well above the thermochemical threshold energy of $\text{CF}_2\text{-CH}_3^+ + \text{F} + \text{e}^-$. The daughter ion is therefore likely to be formed with the release of significant kinetic energy. We comment that, in principle, it should be possible to determine experimentally the *absolute* value of $\Delta_f H^\circ_{298}(\text{CF}_2\text{-CH}_3^+)$ by measuring the kinetic energy release into $\text{CF}_2\text{-CH}_3^+ + \text{F}$ as a function of photon energy,

and extrapolating the linear graph to determine the photon energy at which the kinetic energy release would be zero.³⁸ This procedure would then yield the dissociative ionisation energy, *i.e.* $\Delta_f H^\circ_0$ for the reaction $\text{CF}_3\text{-CH}_3 \rightarrow \text{CF}_2\text{-CH}_3^+ + \text{F} + \text{e}^-$. Unfortunately, whilst this experiment has been successfully employed for the *ground* electronic state of polyatomic cations which are repulsive in the Franck–Condon region (*e.g.* CF_4^+ and SF_6^+),³⁸ we have not been able to yield equivalent data for repulsive, *excited* electronic states.^{10,11} Possible reasons for the failure of such experiments are described elsewhere.^{10,11} We can, therefore, only confirm an experimental upper limit for $\Delta_f H^\circ_{298}(\text{CF}_2\text{-CH}_3^+)$ of 546 ± 11 kJ mol⁻¹.

Above 17 eV, minor ions are observed. The strongest is CF-CH_2^+ which appears with a threshold of 17.1 ± 0.1 eV. Energetically, this minor ion can only form with $\text{HF} + \text{F}$ as neutrals (Table 1). As the direct three-body dissociation $\text{CF}_3\text{-CH}_3 \rightarrow \text{CF-CH}_2^+ + \text{HF} + \text{F} + \text{e}^-$ seems unlikely, we propose a two-step mechanism to form CF-CH_2^+ . The first step involves the loss of a F atom to produce $\text{CF}_2\text{-CH}_3^+$, the second step ($\text{CF}_2\text{-CH}_3^+ \rightarrow \text{CF-CH}_2^+ + \text{HF}$) proceeds *via* a tight transition state and HF elimination. The ion yield curves of CF-CH_2^+ and $\text{CF}_2\text{-CH}_3^+$ support this suggestion, since the increase of the CF-CH_2^+ signal corresponds exactly to the decrease of the $\text{CF}_2\text{-CH}_3^+$ signal. The second step will almost certainly involve a barrier in the exit channel, and could explain why the AE_{298} of CF-CH_2^+ bears no relation to the energy of the dissociation channel $\text{CF-CH}_2^+ + \text{HF} + \text{F} + \text{e}^-$; the former lies *ca.* 1.5 eV higher in energy. Such a three-body dissociation through a sequential two-step mechanism has already been suggested to explain the products of dissociative photoionisation of $\text{CFCl}_2\text{-CH}_3$ ³⁹ and $\text{CHF}_2\text{-CH}_3$.⁴⁰ Above 18 eV, CF-CH_2^+ becomes the dominant ion fragment. Very weak signals due to the minor ions $\text{CF}_2\text{-CH}_2^+$ (mass 64 u) and CH_2F^+ (mass 33 u) are also observed above 16.5 eV. In the latter case, the most likely accompanying neutral fragment is CHF_2 , so these products can only form *via* both H- and F-migration across the C–C bond.

5.2.2 Coincidence ion yields of $\text{CHF}_2\text{-CH}_2\text{F}^+$. The TPEPI-CO spectrum in the energy range 11.8–24.0 eV was measured with an optical resolution of 0.3 nm. The ion yields are shown in Fig. 6. The parent ion appears at lowest energy from the ground ionic state. As the photon energy increases, a C–C bond fragmentation reaction takes place, followed at higher energy by cleavage of a C–F bond. This can be seen in the ion yields for CHF_2^+ , CH_2F^+ , and $\text{CHF-CH}_2\text{F}^+$ or $\text{CHF}_2\text{-CH}_2^+$. As with the 1,1,1 isomer, C–H bond cleavage is not observed. These four major ions are the dominant fragments until 16 eV, when a new reaction channel involving two or more bond cleavages opens, possibly with intra-molecular proton transfer.

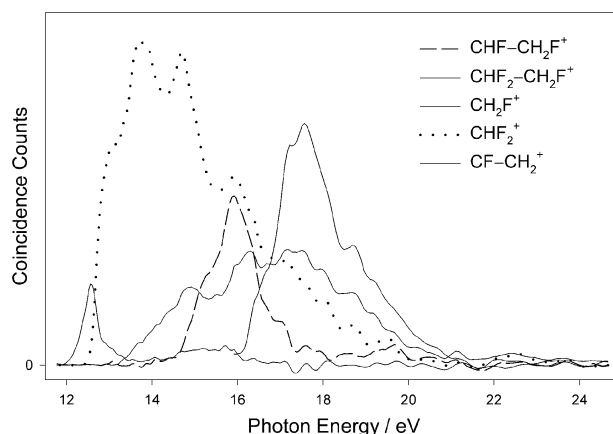


Fig. 6 Coincidence ion yields from $\text{CHF}_2\text{-CH}_2\text{F}$ over the energy range 12–25 eV. The optical resolution is 0.3 nm.

The fragment CF-CH_2^+ gradually becomes the dominant ion in the higher photon energy region, and we note that an ion of mass 45 u was also dominant with $h\nu > 18$ eV for 1,1,1 trifluoroethane (Section 5.2.1). As for $\text{CF}_3\text{-CH}_3$, we have used the procedure of Traeger and McLoughlin³⁰ to convert the AE_{298} of the major fragment ions, determined from an extrapolation of the linear portion of the ion yield to the baseline, into an upper limit for the enthalpy of the unimolecular reaction at 298 K, $\Delta_r H^\circ_{298}$, in order to determine unknown values of enthalpies of formation at this temperature. For the minor ions, we only compare $\text{AE}_{298}(\text{CF-CH}_2^+)$ with $\Delta_r H^\circ_{298}$ for the possible dissociation reactions to infer what the accompanying neutrals may be.

From the onset of ionisation, 11.88 eV, up to *ca.* 12.5 eV, the parent ion forms exclusively, implying that low vibrational levels of the ground state of the parent cation are bound and lie below the first dissociation threshold. The parent ion intensity decreases sharply when the fragmentation channel to produce CHF_2^+ becomes energetically allowed. CHF_2^+ has an AE_{298} of 12.50 ± 0.04 eV, and is the predominant ion from *ca.* 12.8 to 16.0 eV. The AE_{298} can be converted into an upper limit of the enthalpy change for the reaction $\text{CHF}_2\text{-CH}_2\text{F} \rightarrow \text{CHF}_2^+ + \text{CH}_2\text{F} + \text{e}^-$ at 298 K of 12.65 ± 0.04 eV. This value is in excellent agreement with the value of $\Delta_r H^\circ_{298}$, 12.76 eV, derived by us from G2 calculations for the enthalpy of formation of reactants and products of this reaction. The other possible ionic product from cleavage of the C-C bond, CH_2F^+ , has an AE_{298} of 13.19 ± 0.04 eV, corresponding to $\Delta_r H^\circ_{298} \leq 13.34 \pm 0.04$ eV. This latter value is only in reasonable agreement with our G2 calculation for the enthalpy change for the reaction $\text{CHF}_2\text{-CH}_2\text{F} \rightarrow \text{CHF}_2 + \text{CH}_2\text{F}^+ + \text{e}^-$ of 13.08 eV. Both CHF_2^+ and CH_2F^+ form by cleavage of the C-C bond, and are the expected products for dissociation by removing a σ electron from the HOMO of $\text{CHF}_2\text{-CH}_2\text{F}$. As with the 1,1,1 isomer, the good agreement of both energies with theory implies no exit channel barriers or kinetic shifts in either fragmentation channel. Combining these experimental values of $\Delta_r H^\circ_{298}$ with literature values for the enthalpies of formation of CHF_2 (-237 kJ mol⁻¹), CH_2F (-33 kJ mol⁻¹), CH_2F^+ (833 kJ mol⁻¹)²⁹ and CHF_2^+ (604 kJ mol⁻¹),¹⁰ a refined, average enthalpy of formation at 298 K for $\text{CHF}_2\text{-CH}_2\text{F}$ of -671 ± 12 kJ mol⁻¹ is deduced. This value is in excellent agreement with our G2 calculation, -680 kJ mol⁻¹, and other literature values in the range -656 to -665 kJ mol⁻¹.^{16,41}

At a photon energy of 14.51 ± 0.05 eV, corresponding to $\Delta_r H^\circ_{298} \leq 14.65 \pm 0.05$ eV,³⁰ the signal from an ion of mass 65 u increases rapidly. This signal, corresponding to F-atom loss from the parent ion, approximately matches the drop in the ion signal of CHF_2^+ . It is not possible to differentiate the two isomers $\text{CHF-CH}_2\text{F}^+$ or $\text{CHF}_2\text{-CH}_2^+$ in the TOF-MS. G2 calculations predict $\Delta_r H^\circ_{298}$ to be 13.72 eV for the reaction $\text{CHF}_2\text{-CH}_2\text{F} \rightarrow \text{CHF-CH}_2\text{F}^+ + \text{F} + \text{e}^-$ and 12.42 eV for the reaction $\text{CHF}_2\text{-CH}_2\text{F} \rightarrow \text{CHF}_2\text{-CH}_2^+ + \text{F} + \text{e}^-$. Both channels are therefore open at the AE_{298} threshold of 14.51 eV. Formation of the other isomer with mass 65 u, $\text{CF}_2\text{-CH}_3^+$, involves both fission of a C-F bond and H-atom migration, and seems unlikely. The energy of 14.51 eV is close to the onset of the (HOMO - 3) $\tilde{\text{C}}$ excited state of $\text{CHF}_2\text{-CH}_2\text{F}^+$ centred at 15.97 eV, and the yield of this fragment ion follows closely the threshold photoelectron signal of the $\tilde{\text{C}}$ state. Molecular orbital calculations predict that the $\tilde{\text{C}}$ state of $\text{CHF}_2\text{-CH}_2\text{F}^+$ is produced by electron removal from a F $2p\pi$ non-bonding orbital localised predominantly on the CHF_2 group (Section 4.2). It seems likely, therefore, at least near threshold, that $\text{CHF-CH}_2\text{F}^+$ is the dominant component and arises from the dissociation $\text{CHF}_2\text{-CH}_2\text{F} \rightarrow \text{CHF-CH}_2\text{F}^+ + \text{F} + \text{e}^-$. Careful analysis of the ion yield shows a two-step increase, with a second threshold at *ca.* 15.2 eV. It is possible that this second threshold is due either to rapid dissociative ionisation from a different electronic state of the parent ion or to formation of a

different isomer of $\text{C}_2\text{H}_3\text{F}_2^+$; we note that ionisation from the (HOMO - 4) orbital followed by impulsive F-atom loss may lead to significant production of the isomer $\text{CHF}_2\text{-CH}_2^+$. From $\Delta_r H^\circ_{298} \leq 14.65 \pm 0.05$ eV, we determine $\Delta_r H^\circ_{298}(\text{CHF-CH}_2\text{F}^+) \leq 663 \pm 13$ kJ mol⁻¹. However, since the dissociation $\text{CHF}_2\text{-CH}_2\text{F}^+ \rightarrow \text{CHF-CH}_2\text{F}^+ + \text{F}$ has a considerable kinetic energy release (Fig. 7 and Section 5.3), it is likely that the absolute enthalpy of formation of this ion is significantly lower than this value. A G2 calculation, for example, predicts $\Delta_r H^\circ_{298}(\text{CHF-CH}_2\text{F}^+)$ to be 565 kJ mol⁻¹, and Lias *et al.*²⁹ quote 543 kJ mol⁻¹ determined from the proton affinity of CHF=CHF .

As observed in the dissociative photoionisation of other fluorine-substituted ethanes,^{10,11,34} a rapid impulsive mechanism involving cleavage of the C-F bond often occurs when the molecular orbital from which the electron has been removed has mainly F $2p\pi$ lone pair character. If this mechanism is occurring, the fragment ion + F atom will have considerable translational kinetic energy, and can lead to a large difference between the observed dissociative ionisation threshold and the calculated energy of reaction. From the calculated electron densities of the molecular orbitals, and the fact that a large fraction of the available energy is deposited into translation kinetic energy of fragments in the $\text{CHF-CH}_2\text{F}^+$ or $\text{CHF}_2\text{-CH}_2^+ + \text{F}$ decay channel (Table 4), it seems likely that $\text{CHF-CH}_2\text{F}^+$ or $\text{CHF}_2\text{-CH}_2^+$ is produced directly and impulsively from the $\tilde{\text{C}}$ and/or $\tilde{\text{D}}$ excited electronic states of $\text{CHF}_2\text{-CH}_2\text{F}^+$ without prior internal conversion to the ground state. These states of the parent ion are then showing the characteristics of isolated-state behaviour, a phenomenon which is expected in

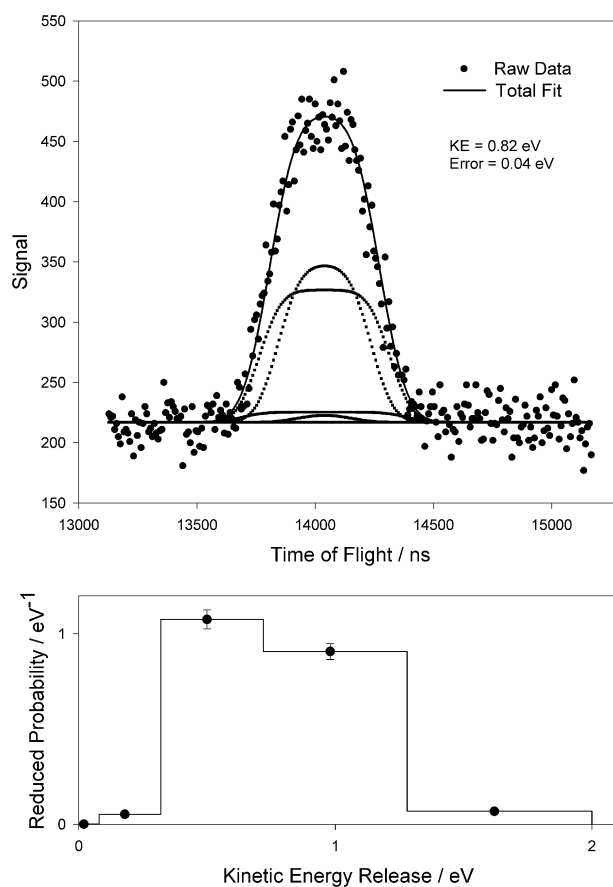


Fig. 7 Coincidence TOF spectra of either $\text{CHF-CH}_2\text{F}^+$ or $\text{CHF}_2\text{-CH}_2^+$ from $\text{CHF}_2\text{-CH}_2\text{F}$ photoionised at 16.02 eV. The solid line gives the best fit to the data, comprised of five contributions ($n = 1-5$) in the basis set for $\varepsilon_n(n)$.²⁷ The reduced probability of each contribution is shown in (b). The fit yields a total mean translational kinetic energy, $(\text{KE})_T$, into the daughter ion + F of 0.82 ± 0.04 eV, which constitutes 51% of the available energy.

Table 4 Mean translation KE releases, $\langle KE \rangle_T$, of the two-body fragmentation of the valence states of $CF_3-CH_3^+$ and $CHF_2-CH_2F^+$

| Parent ion | Fragment ion | $h\nu/eV$ | E_{avail}/eV^a | $\langle KE \rangle_T/eV$ | Fraction ratio ^b | | | |
|---------------|-----------------|--------------------|------------------|---------------------------|-----------------------------|-------------|-----------|------|
| | | | | | Experimental | Statistical | Impulsive | |
| $CF_3-CH_3^+$ | CF_3^+ | 14.50 | 1.34 | 0.13 ± 0.02 | 0.10 | 0.06 | 0.49 | |
| | | 14.95 ^c | 1.79 | 0.32 ± 0.03 | 0.18 | 0.06 | 0.49 | |
| | | 18.99 | 5.83 | 0.48 ± 0.02 | 0.08 | 0.06 | 0.49 | |
| | | 20.16 | 7.00 | 0.58 ± 0.02 | 0.08 | 0.06 | 0.49 | |
| | CH_3^+ | 16.00 | 1.84 | 0.08 ± 0.01 | 0.04 | 0.06 | 0.49 | |
| | | 18.99 | 4.83 | 0.16 ± 0.01 | 0.03 | 0.06 | 0.49 | |
| | | 20.16 | 6.00 | 0.24 ± 0.02 | 0.04 | 0.06 | 0.49 | |
| | | | | | | | | |
| | | $CF_2-CH_3^{+d}$ | | | | | | |
| | $CHF_2-CH_2F^+$ | CHF_2^+ | 13.03 | 0.62 | 0.02 ± 0.002 | 0.03 | 0.06 | 0.30 |
| 13.71 | | | 1.30 | 0.06 ± 0.01 | 0.05 | 0.06 | 0.30 | |
| 14.80 | | | 2.39 | 0.17 ± 0.02 | 0.07 | 0.06 | 0.30 | |
| 16.02 | | | 3.61 | 0.28 ± 0.06 | 0.08 | 0.06 | 0.30 | |
| CH_2F^+ | | 13.71 | 0.61 | 0.02 ± 0.003 | 0.03 | 0.06 | 0.30 | |
| | | 14.80 | 1.70 | 0.13 ± 0.02 | 0.08 | 0.06 | 0.30 | |
| | | 16.02 | 2.92 | 0.11 ± 0.01 | 0.04 | 0.06 | 0.30 | |
| | | 17.64 | 4.54 | 0.16 ± 0.02 | 0.04 | 0.06 | 0.30 | |
| | | | 19.00 | 5.90 | 0.31 ± 0.02 | 0.05 | 0.06 | 0.30 |
| | | $CHF-CH_2F^{+e}$ | 16.02 | 1.61 | 0.82 ± 0.04 | 0.51 | 0.06 | 0.50 |

^a $E_{avail} = h\nu +$ thermal energy of parent molecule at 298K (*i.e.* 0.09 eV) $- AE_{298}$ (daughter ion). ^b Given by $\langle KE \rangle_T/E_{avail}$. ^c Minor component of $CF_2-CH_3^+$ (65 u) in the fit. ^d No measurements made for $CF_2-CH_3^+$ between 14 and 18 eV since its mass is too similar to that of CF_3^+ (69 u) and $CF_2-CH_2^+$ (64 u). ^e May include a very small component of $CHF_2-CH_2^+$.

small cations but is unexpected in polyatomic cations with as many as eight atoms.

At higher photon energies, the ion $CF-CH_2^+$ (possibly with a very small component of ions with mass 44 and 46 u) gradually increases, and for photon energies above *ca.* 17 eV this ion becomes dominant. This ion was also the dominant, minor ion for dissociative photoionisation of CF_3-CH_3 with $h\nu > 18$ eV. The observed AE_{298} of the ion, 16.21 ± 0.05 eV, is significantly higher than the only possible thermochemical reaction energy, 14.76 eV, for the three-body fragmentation $CHF_2-CH_2F \rightarrow CF-CH_2^+ + F + HF + e^-$; fragmentation to $CF-CH_2^+ + F_2 + H + e^-$ at 19.07 eV, or even to $CF-CH_2^+ + 2F + H + e^-$ at 20.71 eV, are both forbidden energetically. As with the 1,1,1 isomer, the increase of the $CF-CH_2^+$ signal roughly matches the decrease of the $C_2H_3F_2^+$ signal. This may imply that $CF-CH_2^+$ is formed *via* a two-step mechanism. First, a fluorine atom is lost from the \check{C} or \check{D} excited states of the parent ion through an impulsive mechanism as described above to form an isomer of $C_2H_3F_2^+$, then formation of $CF-CH_2^+$ occurs from $C_2H_3F_2^+$ *via* a tight transition state, an exit channel barrier, and HF elimination. We note that the difference between the $AE_{298}(CF-CH_2^+)$ and the energy of the dissociation channel $CF-CH_2^+ + HF + F + e^-$ is *ca.* 1.5 eV, the same value as with HF + F elimination from the 1,1,1 isomer (Section 5.2.1).

5.3. Kinetic energy releases

TPEPICO-TOF spectra at a resolution of 8 ns have been recorded for the major fragment ions at photon energies corresponding to the Franck-Condon maxima of the valence states of $CF_3-CH_3^+$ and $CHF_2-CH_2F^+$. These measurements include the parent ion spectra, where the peaks are predicted to be Gaussian in shape with a full width at half maximum (fwhm) proportional to $(MT)^{1/2}/E$, where M is the mass of the parent ion (84 u in this case), T is the temperature (298 K), and E is the extraction field from the interaction region (20 V cm^{-1}).^{42,43} The observation of good fits to the experimental data for both $CF_3-CH_3^+$ and $CHF_2-CH_2F^+$ ³³ with the correct fwhm indicate that spatial focussing is operating correctly in the TOF mass spectrometer.⁴⁴ Fragment ions, however, often have enough translational energy for the TOF peak to be

broadened from that expected for a thermal source. Analysis of the shape of such peaks allows a determination of the kinetic energy release distribution (KERD), and the total mean translational kinetic energy, $\langle KE \rangle_T$, associated with a particular single-bond dissociation. For example, Fig. 7 shows the TPEPICO-TOF spectrum of $CHF-CH_2F^+$ from the \check{C} state of the parent ion $CHF_2-CH_2F^+$ accessed at 16.02 eV. A fit to the peak by a procedure described elsewhere^{26,27} yields $\langle KE \rangle_T = 0.82 \pm 0.04$ eV. The values of $\langle KE \rangle_T$ are sometimes insensitive to the exact form of the KERD, and the error quoted is probably unrealistically low.

$\langle KE \rangle_T$ can be divided by the available energy, E_{avail} , to determine the fraction of the available energy, f_T , being channelled into translational energy of the two fragments. E_{avail} is given by the photon energy plus the thermal energy of the parent molecule at 298 K minus the AE_{298} of the daughter ion. Experimental values of f_T can be compared with those expected if the dissociation follows a pure statistical⁴⁵ or a pure impulsive⁴⁶ model. These two limiting models are described elsewhere.^{10,47} (Note that if dissociation follows the modified-impulsive model,^{47,48} values of f_T may be greater than those calculated for the pure-impulsive model.) Values of $\langle KE \rangle_T$ and f_T are shown in Table 4, together with calculated values of f_T for these two models. Since some of the vibrational wavenumbers of the fragment ions are unknown, statistical values for f_T were calculated according to the lower limit value of $1/(x+1)$, where x is the number of vibrational degrees of freedom in the transition state of the unimolecular reaction.⁴⁹

For CF_3-CH_3 , spectra were measured for the dissociation reaction $CF_3-CH_3^+ \rightarrow CF_3^+ + CH_3$ at photon energies of 14.50, 14.95, 18.99 and 20.16 eV. These energies correspond to the initial formation of the \check{X} , \check{A} , \check{D} and \check{E} states of the parent ion. Spectra were also measured for $CF_3-CH_3^+ \rightarrow CH_3^+ + CF_3$ at 16.00, 18.99 and 20.16 eV, corresponding to formation of the \check{B} , \check{D} and \check{E} states of the parent ion. The experimental and predicted data are shown in the top half of Table 4. For dissociation to CF_3^+ , assuming dissociation always occurs to the ground electronic state of the fragments, low values of f_T are observed at all energies. The value of f_T at 14.95 eV may be anomalously high because there is a minor component of $CF_2-CH_3^+$ signal in the CF_3^+ peak. For dissociation to CH_3^+ , low values of f_T again are observed at all excitation energies.

No measurements could be made for $\text{CF}_3\text{-CH}_3^+ \rightarrow \text{CF}_2\text{-CH}_3^+ + \text{F}$ at the peak of either the $\tilde{\text{B}}$ or $\tilde{\text{C}}$ states of the parent ion, because the fragment ion signal (65 u) shows weak blends from $\text{CF}_2\text{-CH}_2^+$ (64 u) and CF_3^+ (69 u). For $\text{CHF}_2\text{-CH}_2\text{F}$, spectra were also measured for the corresponding dissociation reactions at photon energies corresponding to initial formation of the electronic states of the parent ion. The same pattern for fractional translational energy release is observed. That is, low values of f_{T} , always less than 0.10, are observed at all energies for dissociation to either $\text{CHF}_2^+ + \text{CH}_2\text{F}$ or $\text{CH}_2\text{F}^+ + \text{CHF}_2$. The values are close to that predicted for statistical decay. The signal at mass 65 u due to F-atom loss from dissociative photoionisation of $\text{CHF}_2\text{-CH}_2\text{F}$ is now unblended because CF_3^+ is not observed as a fragment ion. The large value of $\langle \text{KE} \rangle_{\text{T}}$, 0.82 ± 0.04 eV, when the molecule is excited into the $\tilde{\text{C}}$ state of the parent ion was noted in Section 5.2.2. The corresponding value of f_{T} , 0.51, is almost exactly that predicted by the pure-impulsive dissociation model.⁴⁶

Although this pattern of low values of f_{T} for C–C bond and high values for C–F bond cleavage has been observed before in other HFC cations,^{10,11} the absolute values of f_{T} should be treated with some caution. They depend upon the values used for E_{avail} , which themselves depend on a precise determination of the AE_{298} of the daughter ion. Certainly for C–F bond fission, the AE_{298} of the daughter ion may be much higher than the dissociation energy to fragment ion + F. Nevertheless, the high value of f_{T} for F-atom loss from $\text{CHF}_2\text{-CH}_2\text{F}^+$ is consistent with isolated-state behaviour for the $\tilde{\text{C}}$ (and possibly $\tilde{\text{D}}$) states of the parent ion. Dissociation then proceeds along a pseudo-diatomic exit channel of the potential energy surface of the initially excited state. The two atoms of the breaking C–F bond recoil with such force that a relatively large fraction of the available energy is converted into translational energy of the two fragments. Although we were not able to measure f_{T} , we predict the same behaviour for the $\tilde{\text{B}}$ and $\tilde{\text{C}}$ states of $\text{CF}_3\text{-CH}_3^+$. By contrast, the much lower values of f_{T} for C–C bond cleavage in both $\text{CF}_3\text{-CH}_3^+$ and $\text{CHF}_2\text{-CH}_2\text{F}^+$ suggest that the initially-excited state of the parent ion decays non-radiatively by internal conversion to the bound parts of the ground state, then dissociation occurs in a statistical manner from this surface. An alternative explanation is that the C–C bond *does* break in an impulsive manner, but the much lower values of $\langle \text{KE} \rangle_{\text{T}}$ and f_{T} than either impulsive model suggests arise because one of the bond lengths or bond angles in the fragment ion is considerably changed from its value in the parent ion.⁵⁰ Such an *intramolecular* mechanism of fragmentation would result in the daughter ion and/or neutral partner having significant amounts of vibrational energy. Since CF_3^+ , CH_3^+ , and presumably CHF_2^+ and CH_2F^+ , are planar in the isolated ion but approximately pyramidal when located in the parent ion, this model could explain the low values of f_{T} for C–C bond cleavage, with the ν_2 umbrella bending mode of these daughter ions incorporating much of the available energy. From the kinetic energy data alone, therefore, we are not able to distinguish these two mechanisms for how the central C–C bond breaks in either isomer of the trifluoroethane cation.

6. Conclusions

We have recorded the threshold photoelectron and threshold photoelectron photoion coincidence spectra of the two isomers of trifluoroethane, $\text{CF}_3\text{-CH}_3$ and $\text{CHF}_2\text{-CH}_2\text{F}$, in the range 12–24 eV. Ion yield curves have been determined, and the breakdown diagrams are shown elsewhere.³³ The mean translational kinetic energy releases into fragment ions involving a single bond cleavage from selected valence states of $\text{CF}_3\text{-CH}_3^+$ and $\text{CHF}_2\text{-CH}_2\text{F}^+$ have been measured, and compared with the predictions of statistical and pure-impulsive models. *Ab initio* G2 calculations have determined the minimum energies of $\text{CF}_3\text{-CH}_3$ and $\text{CHF}_2\text{-CH}_2\text{F}$ and their cations, with their

geometries optimised at the MP2(full)/6-31G(d) level of theory. The nature of the valence orbitals of both neutral molecules has also been deduced. In addition, enthalpies of formation at 298 K of $\text{CF}_3\text{-CH}_3$, $\text{CHF}_2\text{-CH}_2\text{F}$, and the major and minor ions observed by dissociative photoionisation have been calculated at this level of theory.

Combining experimental and theoretical data, the decay mechanism of the ground and low-lying excited valence states of $\text{CF}_3\text{-CH}_3^+$ and $\text{CHF}_2\text{-CH}_2\text{F}^+$ have been discussed. Both molecules have ground electronic states of the parent cation which are stable only over a narrow range of energies corresponding to the lower vibrational levels. As the photon energy increases, the fractional yield of the parent cation decreases from unity, and C–C bond cleavage produces CF_3^+ and CH_3^+ from $\text{CF}_3\text{-CH}_3$, CHF_2^+ and CH_2F^+ from $\text{CHF}_2\text{-CH}_2\text{F}$. It is assumed that these four ions all turn on at their thermochemical threshold with no activation barrier in the exit channel. We have converted these energy thresholds into upper limits for the enthalpy of the corresponding reactions at 298 K,³⁰ and thus determined new values for the enthalpy of formation at this temperature of $\text{CF}_3\text{-CH}_3$ and $\text{CHF}_2\text{-CH}_2\text{F}$. Only a low fraction of the available energy, $f_{\text{T}} < 0.1$, is channelled into translational energy of the fragment ion and polyatomic neutral.

At higher energy, C–F bond cleavage is associated with electron removal from the (HOMO – 2) and (HOMO – 3) 2π nonbonding orbitals of $\text{CF}_3\text{-CH}_3$. Impulsive dissociation from the $\tilde{\text{B}}$ and $\tilde{\text{C}}$ states of $\text{CF}_3\text{-CH}_3^+$ via C–F bond cleavage then leads to production of $\text{CF}_2\text{-CH}_3^+ + \text{F}$. Although not measured experimentally, we infer that a much larger fraction of the available energy is now channelled into product translation. Decay from the $\tilde{\text{C}}$ and $\tilde{\text{D}}$ states of $\text{CHF}_2\text{-CH}_2\text{F}^+$, formed by electron removal from the F 2π nonbonding (HOMO – 3) and (HOMO – 4) orbitals of the neutral molecule, also leads to C–F bond cleavage, and production of either $\text{CHF-CH}_2\text{F}^+$ or $\text{CHF}_2\text{-CH}_2^+ + \text{F}$. Now a large value of f_{T} is measured experimentally, and confirms that these states display isolated-state behaviour and decay impulsively. It is also likely that the geometry of the daughter ion will not differ significantly from that of the corresponding group in $\text{CHF}_2\text{-CH}_2\text{F}^+$.^{46,47} For both molecules, the AE_{298} of the daughter ion with mass 65 u lies significantly higher in energy than the thermochemical energy of the dissociation channel, so only an upper limit for the enthalpy of formation at 298 K of $\text{CF}_2\text{-CH}_3^+$ and $\text{CHF-CH}_2\text{F}^+$ or $\text{CHF}_2\text{-CH}_2^+$ is determined.

Several examples of minor fragment ions caused by more complicated unimolecular reactions are observed. For both isomers of trifluoroethane, CF-CH_2^+ is observed, and indeed for $h\nu > ca.$ 18 eV this ion is the dominant fragment from dissociative photoionisation of both $\text{CF}_3\text{-CH}_3$ and $\text{CHF}_2\text{-CH}_2\text{F}$. A two-step mechanism, fluorine-atom loss then HF elimination, is suggested to explain its presence.

Acknowledgements

We thank EPSRC for a Postdoctoral Fellowship (WZ), studentships (DJC and DPS), and research grants, including beamtime costs at the Daresbury SRS. RYLC thanks the University of Birmingham for a studentship. We thank Drs Paul Hatherly and Barry Fisher (Reading University) for technical advice on the use of the coincidence apparatus, and Chris Howle for a critical reading of the manuscript.

References

- 1 J. C. Farman, B. G. Gardiner and J. D. Shanklin, *Nature*, 1985, **315**, 207.
- 2 S. Solomon, *Nature*, 1990, **347**, 347.
- 3 R. E. Banks, *J. Fluorine Chem.*, 1994, **67**, 193.
- 4 B. Sukornick, *Int. J. Thermophys.*, 1989, **10**, 553.

- 5 A. R. Ravishankara and E. R. Loveday, *J. Chem. Soc. Faraday Trans.*, 1994, **90**, 2159.
- 6 W. B. DeMore, S. P. Sander, D. M. Golden, R. F. Hampson, M. J. Kurylo, C. J. Howard, A. R. Ravishankara, C. E. Kolb and M. J. Molina, *JPL Publication 97-4, Chemical Kinetics and Photochemical Data for use in Stratospheric Modelling, Evaluation No. 12*, Jet Propulsion Laboratory, Pasadena, CA, 1997.
- 7 J. Barry, H. Sidebottom, J. Treacy and J. Franklin, *Int. J. Chem. Kinet.*, 1995, **27**, 27.
- 8 G. K. Jarvis, K. J. Boyle, C. A. Mayhew and R. P. Tuckett, *J. Phys. Chem. A.*, 1998, **102**, 3219.
- 9 G. K. Jarvis, K. J. Boyle, C. A. Mayhew and R. P. Tuckett, *J. Phys. Chem. A.*, 1998, **102**, 3230.
- 10 Weidong Zhou, D. P. Secombe, R. P. Tuckett and M. K. Thomas, *Chem. Phys.*, 2002, **283**, 419.
- 11 Weidong Zhou, D. P. Secombe and R. P. Tuckett, *Phys. Chem. Chem. Phys.*, 2002, **4**, 4623.
- 12 Weidong Zhou, D. P. Secombe, R. Y. L. Chim and R. P. Tuckett, *Surf. Rev. Lett.*, 2002, **9**, 153.
- 13 V. F. Kalasinsky, H. V. Anjarla and T. S. Little, *J. Phys. Chem.*, 1982, **86**, 1351.
- 14 B. Beagley and D. E. Brown, *J. Mol. Struct.*, 1979, **54**, 175.
- 15 S. Papasavva, K. H. Illinger and J. E. Kenny, *J. Phys. Chem.*, 1996, **100**, 10100.
- 16 Y. Chen, S. T. Paddison and E. Tschuikow-Roux, *J. Phys. Chem.*, 1994, **98**, 1100.
- 17 J. M. Martell and R. J. Boyd, *J. Phys. Chem.*, 1992, **96**, 6287.
- 18 M. R. Zachariah, P. R. Westmoreland, D. R. Burgess, W. Tsang and C. F. Melius, *J. Phys. Chem.*, 1996, **100**, 8737.
- 19 T. Yamada, T. H. Lay and J. W. Bozzelli, *J. Phys. Chem. A.*, 1998, **102**, 7286.
- 20 L. F. Thomas, J. S. Heeks and J. Sheridan, *Z. Elektrochem.*, 1957, **61**, 935.
- 21 S. S. Chen, A. S. Rodgers, J. Chao, R. C. Wilhoit and B. J. Zwolinski, *J. Phys. Chem. Ref. Data*, 1975, **4**, 441.
- 22 P. Sauvageau, J. Doucet, R. Gilbert and C. Sandorfy, *J. Chem. Phys.*, 1974, **61**, 391.
- 23 J. M. Simmie and E. Tschuikow-Roux, *Int. J. Mass Spectrom. Ion Phys.*, 1971, **7**, 41.
- 24 L. A. Curtiss, K. Raghavachari, G. W. Trucks and J. A. Pople, *J. Chem. Phys.*, 1991, **94**, 7221.
- 25 P. A. Hatherly, D. M. Smith and R. P. Tuckett, *Z. Phys. Chem.*, 1996, **195**, 97.
- 26 I. Powis, P. I. Mansell and C. J. Danby, *Int. J. Mass Spectrom. Ion Phys.*, 1979, **32**, 15.
- 27 G. K. Jarvis, D. P. Secombe and R. P. Tuckett, *Chem. Phys. Lett.*, 1999, **315**, 287.
- 28 M. W. Chase, *J. Phys. Chem. Ref. Data, Monogr.*, 1998, **9**.
- 29 S. G. Lias, J. E. Bartmess, J. F. Liebman, J. L. Holmes, R. D. Levin and W. G. Mallard, *J. Phys. Chem. Ref. Data, Suppl.* 1988, **17**.
- 30 J. C. Traeger and R. G. McLoughlin, *J. Am. Chem. Soc.*, 1981, **103**, 3647.
- 31 <http://webbook.nist.gov/>.
- 32 C. R. Brundle, M. B. Robin, N. A. Kuebler and H. Basch, *J. Am. Chem. Soc.*, 1972, **94**, 1451.
- 33 D. J. Collins, PhD Thesis, University of Reading, UK, 2004.
- 34 I. G. Simm, C. J. Danby, J. H. D. Eland and P. I. Mansell, *J. Chem. Soc., Faraday Trans. 2*, 1976, **72**, 426.
- 35 J. A. Blush, P. Chen, R. T. Wiedmann and M. G. White, *J. Chem. Phys.*, 1993, **98**, 3557.
- 36 B. Ruscic, J. V. Michael, P. C. Redfern, L. A. Curtiss and K. Raghavachari, *J. Phys. Chem. A.*, 1998, **102**, 10889.
- 37 G. A. Garcia, P. M. Guyon and I. Powis, *J. Phys. Chem. A.*, 2001, **105**, 8296.
- 38 R. Y. L. Chim, R. A. Kennedy, R. P. Tuckett, W. Zhou, G. K. Jarvis, D. J. Collins and P. A. Hatherly, *J. Phys. Chem. A.*, 2001, **105**, 8403.
- 39 S. Y. Chiang, T. T. Wang, J. S. K. Yu and C. Yu, *Chem. Phys. Lett.*, 2000, **329**, 185.
- 40 T. Heinis, R. Bar, K. Borlin and M. Jungen, *Chem. Phys.*, 1985, **94**, 235.
- 41 J. R. Lacher and H. A. Skinner, *J. Chem. Soc. A.*, 1968, 1034.
- 42 J. L. Franklin, P. M. Hierl and D. A. Whan, *J. Chem. Phys.*, 1967, **47**, 3148.
- 43 J. H. D. Eland, *Int. J. Mass Spectrom. Ion Phys.*, 1972, **8**, 143.
- 44 W. C. Wiley and I. H. Maclaren, *Rev. Sci. Instrum.*, 1955, **26**, 1150.
- 45 C. E. Klots, *J. Chem. Phys.*, 1973, **58**, 5364.
- 46 K. E. Holdy, L. C. Klots and K. R. Wilson, *J. Chem. Phys.*, 1970, **52**, 4588.
- 47 D. P. Secombe, R. Y. L. Chim, G. K. Jarvis and R. P. Tuckett, *Phys. Chem. Chem. Phys.*, 2000, **2**, 769.
- 48 G. E. Busch and K. R. Wilson, *J. Chem. Phys.*, 1972, **56**, 3626.
- 49 J. L. Franklin, *Science*, 1976, **193**, 725.
- 50 R. C. Mitchell and J. P. Simons, *Discuss. Faraday Soc.*, 1967 **44**, 208.